### **RESEARCH PAPER**



# Void size distribution and hydraulic conductivity of a binary granular soil mixture

C. S. Chang<sup>1</sup> • T. T. Ma<sup>1</sup>

Received: 16 September 2022 / Accepted: 14 July 2023 © The Author(s), under exclusive licence to Springer-Verlag GmbH Germany, part of Springer Nature 2023

#### **Abstract**

Permeability of binary mixtures of soils is important for several industrial and engineering applications. Previous models for predicting the permeability of a binary mixture of soils were primarily developed from Kozeny–Carman equation with an empirical approach. The permeability is predicted based on an equivalent particle size of the two species. This study is aimed to develop a model using a more fundamental approach. Instead of an equivalent particle size, the permeability is predicted based on the bimodal void sizes of the binary mixture. Because the bimodal void sizes are not available as commonly measured physical properties. We first develop an analytical method that has the capability of predicting the bimodal void sizes of a binary mixture. A permeability model is then developed based on the bimodal void sizes of the binary mixture. The developed permeability model is evaluated by comparing the predicted and experimentally measured results for binary mixtures of glass beads, crush sand, and gravel sand. The findings can contribute to a better understanding of the important influence of pore structure on the prediction of permeability.

Keywords Bi-dispersed granular packing · Bimodal void distribution · Partial void ratios · Permeability

#### 1 Introduction

Fluid flow in soils is an important consideration on the design, construction, and stability of many civil engineering structures. A reliable analytical model for predicting permeability of soils is a critical element in geotechnical engineering analysis [1, 6, 15, 28].

Among the various analytical formulas for estimating permeability for soils, the Kozeny–Carman equation is the most popularly used, which was derived from Poiseuille's law and considered the pore space in soil as a bunch of capillary tubes [3, 8, 9, 13, 16, 17, 24, 28]. A commonly used form is as follows:

$$k = \frac{1}{5} \left(\frac{d}{SF}\right)^2 \frac{n^3}{(1-n)^2} \tag{1}$$

where SF = particle shape factor (round particles: 6.0–6.6; angular particles: 7.7–8.4), n is the porosity and d is the

Published online: 03 September 2023

particle size of the packing [9, 14, 17, 26]. It has been reported that the prediction of Kozeny–Carman equation is in good agreement with the measured permeability for mono-sized packings of glass beads and for packings of uniformly graded sand [37, 46].

However, it has been found that Eq. (1) does not provide good predictions for the permeability of natural soils or geomaterials, which are usually mixtures of two or more soils of different particle sizes (e.g., silty sand and clayey sand). For general soils with wide size distribution, a number of empirical formulas have been proposed, for example, by Hazen [20], Terzaghi and Peck [40], the equation of the Naval Facilities Engineering Command [32], Chapuis [12], Riva et al. [34], Wang et al. [44], etc. In these empirical equations, the d in Eq. (1) is usually replaced by an equivalent particle size, for example,  $d_{10}$  (particle size at 10% pass by mass obtained from the particle-size distribution curve).

Rosas et al. [36] collected 20 empirical equations and compared the calculated and measured permeabilities for hundreds of soil samples from different environments in global locations. They reported that the calculated permeability using empirical equations is poorly correlated to the



C. S. Chang chang@ecs.umass.edu

University of Massachusetts, Amherst, MA, USA

measurements with errors over 500%. The discrepancies are expected, since an empirical equation is usually derived from data of given soil types; it cannot be applicable universally to all types of soil. Thus, these empirical equations are not suitable for accurate prediction for widely graded soil.

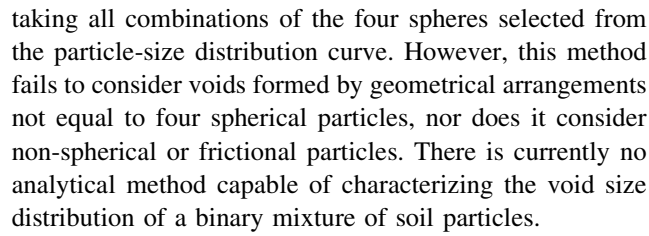
The Kozeny–Carman equation can also be used to calculate the permeability of a bi-dispersed packing by using an equivalent size  $d_{\rm eq}$ . However, it is not an easy task to determine the value of  $d_{\rm eq}$ , which varies with the particle sizes, packing porosity and fines content of the binary mixture. Studies on the value of  $d_{\rm eq}$  for various binary mixtures can be found in the work by Thies-Weesie et al. [42], Mota et al. [31], Lee and Koo [25], Choo et al. [14]. However, the approach of determining an equivalent size  $d_{\rm eq}$  is still empirical. Thus, the empirical equation derived from the experimental data for one type of soil cannot be applied to all types of soil. Hence, it seems necessary to take a more fundamental approach rather than an empirical approach.

Several investigators utilized void size distribution (VSD) to predict permeability [7, 13, 19, 22, 23, 29]. This modelling approach is more fundamental because the cross-sectional area of capillary tubes is directly estimated from the void sizes and void distribution, instead of particle sizes.

In order to use this approach to predict permeability, an accurate void size distribution (VSD) is required for each binary mixture. The void size distribution (VSD) data are traditionally measured by mercury intrusion porosimeter or interpreted by experimentally determined soil—water retention curves [2, 19, 21]. More recently, Koohmishi and Azarhoosh [29] attempted to determine the pore size distribution from two dimensional images of the material. O'Sullivan et al. [33], Mokwa and Trimble [29] and Taylor et al. [39] assessed the pore structure for sandy soils using computer simulation method and computer tomography.

It is noted that the void size distribution varies from mixture to mixture, which is a complex function of soil composition and soil type. Although, for each binary mixture, the VSD can be measured using mercury porosimeter, retention curves, computer tomography or possibly computer simulation method, these methods are practically cumbersome. Furthermore, the measured VSD is only for a specific binary mixture of a given fines content, thus, the process of calculating permeability cannot be regarded as a predictive method. Therefore, an analytical model is needed to estimate and characterize the void size distribution of *any* binary mixture of granular soil.

Recently, Fujikura [18] proposed an analytical method for estimating the void size by assuming that each void is formed by four spheres. The VSD can then be computed by



In this paper, we aim to develop a more precise analytical method to determine the void size distribution of a binary mixture through the theory of excess volume potential proposed in the work by Chang and Deng [11], and Chang [10], which prescribes the porosities associated with each species of the binary mixture. Making use of the excess volume potential, we then develop an analytical method for predicting the bimodal VSD for the binary mixture. Utilizing the bimodal VSD, we formulate a permeability model for the binary mixtures based on Darcy's and Poiseuille's law and estimate the size of capillary tubes directly from the viewpoint of pore structure. Finally, the derived model is evaluated by comparing the predicted and measured permeabilities of various types of binary mixtures for glass beads, crush sand, and gravel sand.

# 2 Void size distribution for bi-dispersed granular packing

# 2.1 Concept of partial void ratios for a bidispersed packing

Based on computer simulation results by Roozbahani et al. [35], a typical void size distribution for a uniform packing (i.e., mono-sized packed spheres) is shown in Fig. 1. The distribution of the void size tends to concentrate towards smaller void sizes, yielding a positively skewed distribution. The horizontal axis represents the ratio of void size to the particle size of spheres. For this packing, the mean

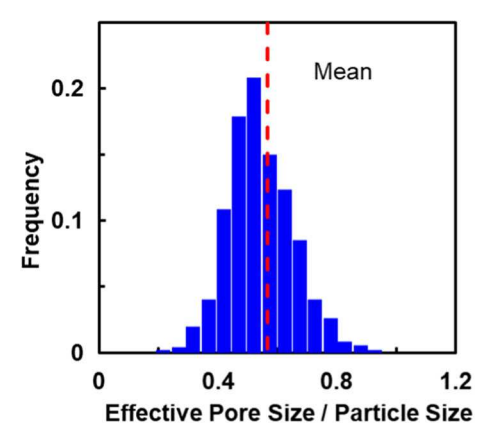


Fig. 1 Void size distribution for a mono-sized packing of spheres (data from Roozbahani et al.[35])



value of this ratio is 0.567, which is found to be equal to the void ratio *e* of the packing (*e* is defined as the ratio of void volume/solid volume of the packing). Thus, the mean void size can be obtained by multiplying the void ratio and the solid particle size of the packing.

A bi-dispersed packing consists of large and small particles. The void ratio of the binary mixture varies with its fines content  $f_c$  (i.e., volume fraction of small particles). A typical variation of void ratio is shown by circular symbols in Fig. 2. The concept of inter-granular and matrix void ratios is commonly used to describe the characteristics of packing structures of binary mixtures.

At  $f_c = 0$ , the void ratio of the mono-sized packing of large particle (or skeleton void ratio) is denoted as  $e_1^0$ . For a binary mixture with a low fines content, the fine particles fill in the void space between large particles, but do not alter the packing structure of large particles (see the insert in left of Fig. 2). Thus  $e_1^0$  can be used to estimate the void ratio,  $e_I$ , of a packing with a low fines content  $f_c$  [41]:

$$e_I = e_1^0 y_1 - y_2 \tag{2}$$

where  $y_1$  and  $y_2$  are the solid volume fractions of the large and small particles respectively (note:  $y_1 = 1 - y_2$ ). Subscript 1 refers to large particles and 2 refers to small particles. The solid volume fraction of small particles  $y_2$  is also termed as fines content  $f_c$ .

On the other hand, at  $f_c = 1$ , the void ratio of the monosized packing of small particles (or matrix void ratio) is denoted as  $e_2^0$ . For a binary packing with a high fines content, the large particles are isolated and embedded in the matrix of small particles. Consider the embedded large particles, which replace THE volume of small particles, but do not alter the packing structure of small particles (see insert in the right of Fig. 2). Thus,  $e_2^0$  can be used to estimate the void ratio,  $e_M$ , of a packing with high fines content [27], given by

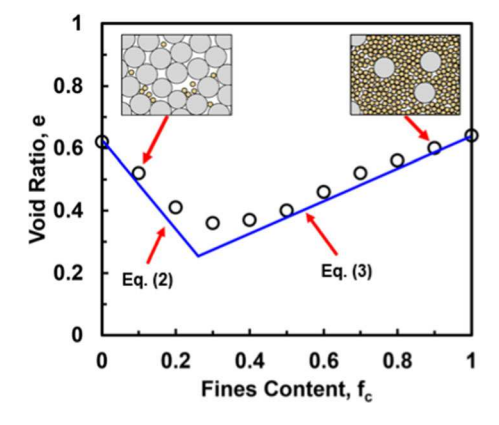


Fig. 2 Void ratio of binary mixtures of silica sands (Data from Yilmaz [45])

$$e_M = e_2^0 y_2 \tag{3}$$

As shown in Fig. 2, for a packing with low fines content (< 5%), the void ratio  $e_I$  of the packing can be approximated by the inter-granular void ratio calculated from Eq. (2). In this range of low fines content, the voids are primarily formed by large particles. The mean void size can be estimated by  $e_I v_1^g$ . The voids formed by small particles are negligible, since the small particles are located in the voids between large particles.

On the other hand, for a packing with high fines content (> 95%), the void ratio of the packing  $e_M$  can be approximated by the matrix void ratio from Eq. (3). In this range of fines content, the voids are primarily formed by small particles. The mean void size can be estimated by  $e_M v_2^g$ . The voids formed by large particles are negligible, since the large particles are isolated embedded.

However, at the middle range of fines content (between 5 and 95%). The void size is bimodal; the large voids are formed among large particles, and the small voids are formed among small particles. Although the overall void ratio of a packing mixture is known, there is no method for calculating the two different void sizes associated with each species of particles.

In order to calculate the two different void sizes associated with each species of particles, a useful view is to consider the volume of a particle packing being partitioned into cells (e.g., Voronoi tessellation). Each cell consists of a solid particle of volume  $v_i^g$  (i = 1, 2 for particles of both species) and its associated void space. The volume of the associated void space is  $e_i^m v_i^g$ , with  $e_i^m$  defined as the void ratio of the mth cell of the ith species. The mth cell volume is  $(e_i^m + 1)v_i^g$ . Given that the overall space of a packing can be divided into Voronoi cells, there are  $N_i$  particles for the ith species. The sum of all cell-volumes is equal to the overall volume V of the packing.

$$V = \sum_{m=1}^{N_1} (1 + e_1^m) v_1^g + \sum_{m=1}^{N_2} (1 + e_2^m) v_2^g$$
 (4a)

Let the partial void ratio  $e_i$  be defined as the mean void ratio for all cells of the ith species. Then Eq. (4a) can be written as

$$V = N_1(1 + e_1)v_1^g + N_2(1 + e_2)v_2^g; e_i = \frac{1}{N_i} \sum_{m=1}^{N_i} e_i^m$$
 (4b)

In Eq. (4b), the total volume is the sum of void volume and solid volume (i.e.,  $V = V_v + V_s$ ), where the solid volume of the packing  $V_s = N_1 v_1^g + N_2 v_2^g$ , and the total void volume  $V_v = eV_s$ . Furthermore, by replacing the particle number  $N_i$  in Eq. (4) to the solid volume fractions (i.e.,  $y_1 = N_1 v_1^g / V_s$ ,  $y_2 = N_2 v_2^g / V_s$ ), the mixture void ratio e can



be expressed as the volume average of two partial void ratios,  $e_1$  and  $e_2$ , of each species.

$$e = y_1 e_1 + y_2 e_2 \tag{5}$$

As previously mentioned, for a mono-sized packing the void size can be estimated from the solid particle size multiplied by void ratio. For a binary packing, the bimodal mean void sizes can be estimated from the partial void ratios by  $e_1v_1^g$  and  $e_2v_2^g$ . The measured two groups of void sizes change in a complex fashion with fines content. As schematically shown in Fig. 3, the void sizes evolute in magnitude with fines content. With an increase of fines content, the large void sizes decrease but the small void sizes increase. Also, the volume fractions of the two void sizes varies with fines content. This trend of void size evolution is consistent with that observed from porosimeter [5].

### 2.2 Prediction of the partial void ratios of a bidispersed packing

As described in the previous section, the bimodal void sizes in a bi-dispersed particle packing can be obtained from the partial void ratios  $e_1$  and  $e_2$  of each species. However, the partial void ratios cannot be measured directly from the specimen of a binary mixture, because the particles of different species are mixed and randomly distributed in the sample space. In order to obtain the partial void ratios  $e_1$  and  $e_2$  for each species using the Voronoi tessellation method describe in Eqs. (4) and (5), it is necessary to know the geometric information of the packing structure at

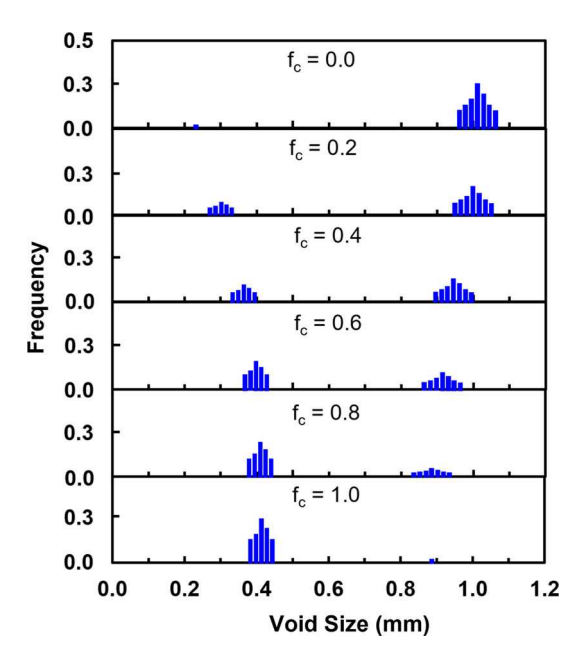


Fig. 3 A schematic plot for the bimodal void size distribution of a bidispersed packing mixture at various fines contents

microscale level, so that a statistical analysis of the Voronoi cell structure can be performed.

A statistical analysis is not feasible, because the detailed packing structure can only be obtained by CT scanning or by computer simulation method. CT scanning is expensive and not practical. The computer simulation does not realistically represent the physical material. Furthermore, both methods are limited to a small range of problems due to the incapacity of handling the required resolution for binary mixtures with large contrast of particle sizes.

Another way to study the partial void ratios is through Euler's theory of homogeneous function [11, 38]. For a bidispersed packing with volume V which consists of  $N_1$  large particles and  $N_2$  small particles, the volume of the packing is a homogeneous function of the first degree, thus can be expressed as

$$V(N_1, N_2) = N_1 \left(\frac{\partial V}{\partial N_1}\right) + N_2 \left(\frac{\partial V}{\partial N_2}\right) \tag{6}$$

Comparing this equation with Eq. (4b), the value

$$\partial V_{\partial N_i} = (1 + e_i)v_i^g$$
.

Thus, the partial void ratio  $e_i$  can be obtained by knowing the change of packing volume due to a small change of particle number  $N_i$ . Applying this definition of partial void ratio, then Eqs. (6) and (5) can lead to the following expressions for the particle void ratios of the two species [36].

$$e_1 = e - f_c \frac{\partial e}{\partial f_c}; \quad e_2 = e + (1 - f_c) \frac{\partial e}{\partial f_c}$$
 (7)

Using this equation, the partial void ratios can be obtained from the test results that provide the relationship between the void ratio and the fines content

$$(i.e., \partial e/\partial f_c)$$

of the soil mixture. Studied from the characteristics of partial void ratios, Chang [10] has developed a concept of excess volume potential, which is a function that characterizes the difference between the partial void ratio  $e_i$  of the packing mixture and the void ratio of the mono-sized packing  $e_i^0$  due to interaction of species. An analytical method was derived, based on the theory of thermodynamics, for the prediction of  $e_1$  and  $e_2$  of a bi-dispersed packing of any given fines content. This model has been verified to be an effective and reliable particle packing model, which can predict the void ratio of a bi-dispersed packing of any given fines content based on the void ratios of the two mono dispersed packings of both species. The model is briefly summarized in Appendix 1.



### 2.3 Prediction of the bi-modal void sizes of a bidispersed packing

The section describes how the mean bi-modal void sizes are determined from the partial void ratios  $e_1$  and  $e_2$  for a binary packing of a given fines content. Let the solid particle volumes be denoted by  $v_1^g$  for a large particle and  $v_2^g$  for a small particle. The mean void volumes  $v_1^v$  and  $v_2^v$  respectively for the large and the small particles can be obtained by

$$v_1^{\text{v}} = e_1 v_1^{\text{g}}; \quad v_2^{\text{v}} = e_2 v_2^{\text{g}}$$
 (8)

Accordingly, the void sizes  $d_i^{\text{v}}(i=1,2)$  associated with each species can be estimated by a dimensional analysis  $(d_i^{\text{v}})^3 = e_i(d_i^g)^3$ .

In addition to the void sizes, we are also interested in knowing the volume fractions of  $v_1^{\rm v}$  and  $v_2^{\rm v}$  for the two species. It is noted that the volume fractions of the voids are different from that of the solid particles for the two species. The volume fractions of the solid particles for the two species are defined by  $y_i = \frac{N_i v_s^g}{V_s} (i = 1, 2)$  where the total solid volume  $V_s = N_1 v_1^g + N_2 v_2^g$ . Correspondingly, the total void volume is  $V_v = N_1 v_1^g + N_2 v_2^v$ , and the volume fractions of the voids  $x_i$  are defined by

$$x_i = \frac{N_i v_i^{\mathsf{v}}}{V_{\mathsf{v}}} \tag{9}$$

Expressing the void volume  $v_i^{\rm v}$  in terms of the partial void ratios of the mixture  $e_i = v_i^{\rm v}/v_i^{\rm g}$ , using the void ratio e in Eqs. (5), (9) becomes

$$x_{i} = \frac{e_{i}}{e} y_{i} \tag{10}$$

As an example, experimental results by Choo et al. [12] on crushed sand mixtures of two different size ratios are used:  $d_1 = 1.09$  mm and  $d_2 = 0.43$  mm  $(d_1/d_2 = 2.53)$  and  $d_1 = 1.09$  mm and  $d_2 = 0.15$  mm  $(d_1/d_2 = 7.1)$ . The mono sized packing void ratio is 0.8879 for particle size 1.09 mm, 0.8395 for particle size 0.43 mm, and 0.8213 for particle size 0.15 mm.

The predicted void ratio e of the binary mixtures for various fines contents are shown in Fig. 4a and b. The predicted void ratio of the mixture in solid line is compared with the experimental results in symbols. At point A, the void ratio of the mixture is lowest denoted as  $e_{\rm opt}$ . The corresponding fines content is denoted as optimum fines content  $f_{\rm opt}$ . For a packing sample with fines content less than  $f_{\rm opt}$ , the packing structure is dominant by large particles with small particles filled in the voids between large particles. On the other hand, for a sample with fines content more than  $f_{\rm opt}$ , the packing structure is dominant by small

particles with the large particles embedded in the matrix of small particles.

The predicted values of  $e_1$  and  $e_2$  vary with fines content are also shown in Fig. 4a and b. It is noted that Eq. (5) is satisfied. The general pattern of the curves is similar for the two different size ratios. The partial void ratios,  $e_1$  and  $e_2$ , are negatively correlated, i.e., one decreases while the other increases. At the optimum point, the partial void ratios  $e_1 = e_2$ .

It is noted that, for the case in Fig. 4b, the value of  $e_2$  is negative at low fines content. From the Euler's equation (i.e., Eq. (6)), the magnitude of  $e_2$  is related to the increase of packing void volume due to an increase of the number of small particles. A negative value of  $e_2$  means that, when the particles are sufficiently small, it would fill in the void space between large particles. This does not increase the total void volume of the packing mixture. Instead, the small particle occupies the void space and decreases the total void volume of the mixture, resulting in a negative value.

As the fines content increases, some small particles may wedge between two large particles increasing the void volume of the packing mixture. However, the magnitude of increased void volume is less than the decreased void volume due to the occupancy of the small particles. Thus, the overall  $e_2$  may still be negative. As the fines content continues to increase, the filled small particles tend to cluster and form layers between large particles, resulting a continued increase of  $e_2$ . At point A, the voids between large particles are fully filled (i.e., optimum fines content  $f_{\text{opt}}$ ). When fines content is higher than  $f_{\text{opt}}$ , more large particles are separated by small particles, and the packing structure is starting to be dominant by small particles. Further increase of fines content makes the large particles isolate and embedded in the matrix of small particles. At fines content approaches one,  $e_2$  is increased to the value of the mono-sized  $e_2^0$  while  $e_1$  approaches zero.

Observed from Fig. 4a and b, it is noted that  $e_1 > 0$  occurs for all fines contents, but  $e_2 > 0$  occurs only for the range of higher fines content. At low fines contents, two conditions can be observed: (1)  $e_2 > 0$  when the size ratio  $d_1/d_2$  is small (see Fig. 4a), (2)  $e_2 < 0$  when the size ratio  $d_1/d_2$  is large (see Fig. 4b). The methods of interpreting void sizes are considered for the two different conditions:

- (1)  $e_2 > 0$ , the mean void volumes  $v_1^{v}$  and  $v_2^{v}$  can be calculate from Eq. (8). The volume fraction of voids  $x_i$  can be obtained from Eq. (9).
- (2)  $e_2 < 0$ ,  $v_2^{\rm v} = 0$ , and  $v_1^{\rm v} = ev_1^{\rm g}$ . In this case, the small particles are insignificant in amount and free-to-move rather than packed in the void spaces of large particles. Thus, there exists no matrix of small particles, and no void volume can be considered as formed by the species of small particles (i.e.  $v_2^{\rm v} = 0$ ).



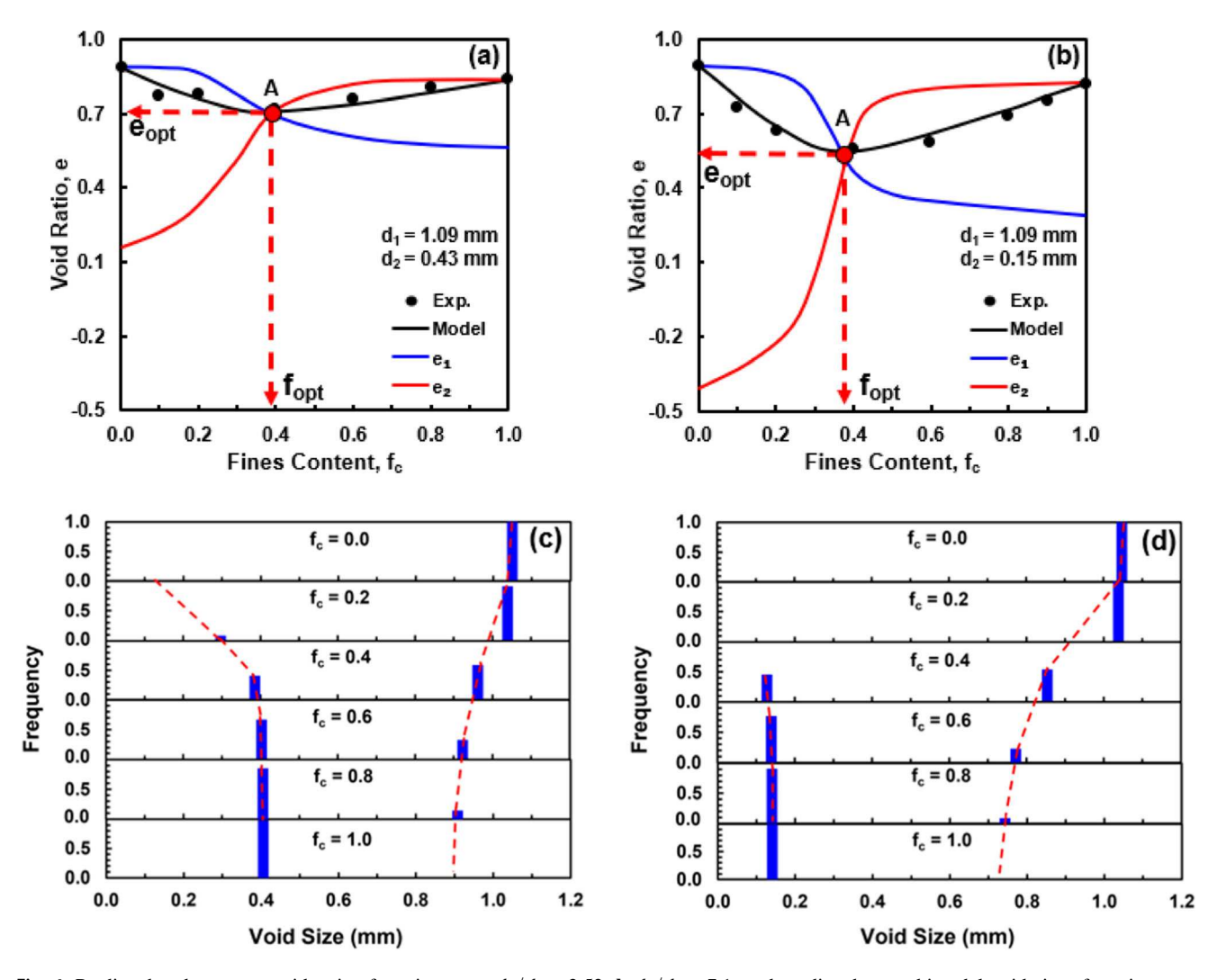


**Fig. 4** Predicted and measure void ratios for mixtures **a**  $d_1/d_2 = 2.53$ , **b**  $d_1/d_2 = 7.1$ , and predicted mean bimodal void sizes for mixtures **c**  $d_1/d_2 = 2.53$ , **d**  $d_1/d_2 = 7.1$  (Data from Choo et al. [14])

The effect of small particles is simply a reduction of the void volume associated with large particles  $v_1^v$ . Thus,  $v_1^v$  is modified by subtracting the voids occupied by the small particles, i.e.,  $v_1^v = (y_1e_1 + y_2e_2)v_1^g$  with  $e_2$  being negative. Applying Eq. (5),  $v_1^v = ev_1^g$ , in which e is the void ratio of mixture as shown in Eq. (5). The volume fraction of voids  $x_i$  can be obtained from Eq. (9).

Using Eqs. (8) and (10), the evolution of the two mean void sizes with varying fines content is shown in Fig. 4c and d. The general pattern of the evolution is similar to that in Fig. 2 described in the previous section.

# 2.4 Prediction of the permeability of a bidispersed packing

One of the pioneer methods used to model flow and transport in porous media is based on the concept of flow in capillary tubes. In this approach, the complex structure of irregular pore space in porous media is replaced with a bundle of tortuous capillary tubes of various sizes. Using Darcy's law and the Poiseuille formula for capillary tube [4, 15, 16, 30], the intrinsic permeability of a bundle of tortuous tubes of the same radius R is given by

$$k = \frac{c}{8\tau} R^2 n \tag{11}$$

in which n is the porosity, c is shape factor and  $\tau = (L_e/L_s)^2$  is the tortuosity, the ratio of effective flow path length  $L_e$  to sample length  $L_s$  [4]. The Kozeny–Carman equation shown in Eq. (1) is derived from Eq. (11) by assuming a connection between the radius of tube R and



the particle size D using the concept of a hydraulic radius for a packing of uniform spheres [8, 24]. Thus, Eq. (11) is more fundamental than the Kozeny–Carman equation.

For the case (2) shown above (i.e.,  $e_2 < 0$ ), the small particles in the voids between the primary matrix do not carry effective stress and are free to move. There are two situations that may occur during the permeability test, which will change the pore structure significantly. Thus, the two situations need to be considered separately.

- (a) Non-percolation condition. These small particles are free to move within the void but cannot transport to other voids of sample, because the inter-void connections are narrower than the particle or the seepage force is not sufficiently large.
- (b) Percolation condition. These small particles transport from void to void by seepage force and settle to the bottom of the sample as schematically shown in Fig. 5a, since the inter-void connections within the primary matrix are large enough.

### 2.4.1 Permeability of a bi-dispersed packing (nonpercolation condition)

We attempt to relate the radius of tube R in Eq. (11) directly to the pore structure by knowing the bimodal mean void sizes and their volume fractions of a packing. Since the bimodal voids are randomly distributed in the granular packing, the pore structure can be viewed as a bundle of tortuous tubes of the same size R. Each tortuous tube is formed by connected voids through the sample length. The large voids and small voids are randomly connected in a serial connection. Thus, the effective void size  $d^{V}$  can be computed by

$$\frac{1}{d^{\mathsf{V}}} = \frac{x_1}{d_1^{\mathsf{V}}} + \frac{x_2}{d_2^{\mathsf{V}}} \tag{12}$$

The value of  $R = d^{v}/2$ .

For the non-percolation condition, as mentioned previously, when  $e_2 > 0$ , the mean void volumes  $v_1^{\rm v}$  and  $v_2^{\rm v}$  can be calculated from Eq. (8). When  $e_2 < 0$ , the volume of voids for the two species,  $v_2^{\rm v} = 0$ , and  $v_1^{\rm v} = e v_1^{\rm g}$ . The effective void size and the permeability of the packing can be calculated from Eqs. (8), (11) and (12).

The value of  $c/(8\tau)$  in Eq. (11) is related to the tortuosity and particle shape, which can be back calculated from the measured permeability for each sample with a given fines content. It was found that the variation of  $c/(8\tau)$  with respect to fines content is insignificant for a given type of binary mixture. This feature will be discussed later.

# 2.4.2 Permeability of a bi-dispersed packings (percolation condition)

For the percolation condition, the permeability of the granular packing is calculated based on the segregated packing structure. Note that, before the particle percolation occurs due to fluid flow, the packing has a fines content  $y_2$ . Due to percolation, we assume that all small particles transport to and fill the lower part of the sample  $(h_b)$ . Thus, the upper part of the sample in Fig. 5a  $(h_a)$  has a zero fines content, i.e.,  $f_a = 0$ , and the fines content of the lower part of the sample is equal to the optimum fines content  $f_{\text{opt}}$  the point A shown in Fig. 5b.

The relative thickness of  $h_a$  and  $h_b$  are dependent on the initial fines content  $y_2$  of the sample, which can be calculated by

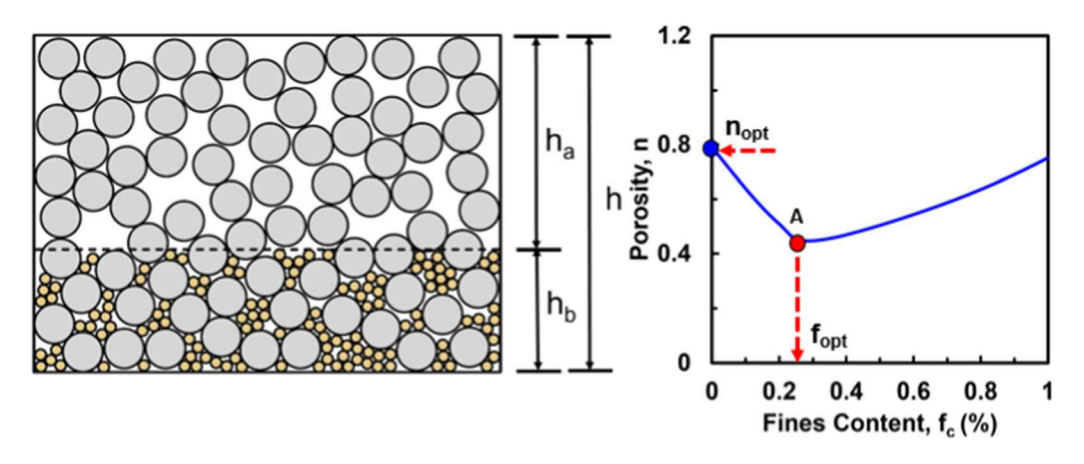


Fig. 5 Schematic diagram of particle segregation in a bi-dispersed sample for permeability test. On the right is the porosity characteristic for the lower part of the bi-dispersed mixtures



$$y_2 h = f_a * h_a + f_{\text{opt}} * h_b \tag{13}$$

since  $f_a = 0$ , thus

$$h_b/h = y_2/f_{\text{opt}}$$
 and  $h_a/h = 1 - (y_2/f_{\text{opt}})$  (14)

Similarly, we calculate the porosities of the upper and lower parts of the sample. The porosity of the mixture is denoted as n, which is related to void ratio by e = n/(1-n). At a given fines content  $y_2$ , the porosity n is known. We assume that the total volume of the sample is not changed after particle percolation. Since the porosity is  $n_{opt}$  for the lower part of the sample, which is fully filled with small particles, the porosity of the upper part  $n_a$  can be computed by

$$nh = n_a h_a + n_{\text{opt}} h_b \quad \text{or} \quad n_a = \frac{n - n_{\text{opt}}(h_b/h)}{h_a/h} \tag{15}$$

After substituting Eq. (14) into Eq. (15), the porosity of the upper part sample is

$$n_a = \frac{n - n_{\text{opt}} \left( y_2 / f_{\text{opt}} \right)}{1 - \left( y_2 / f_{\text{opt}} \right)} \tag{16}$$

With the thickness and porosities described above for the upper and lower part of the sample, the corresponding permeabilities  $k_a$  and  $k_b$  for the two parts can be calculated. The upper part of the sample is a mono-size packing with a void ratio  $e_a = n_a/(1-n_a)$ , and the mean void volume  $v_1^{\rm V} = e_a v_1^{\rm g}$ . Thus, the permeability  $k_a$  can be determined from Eq. (11). The lower part of the sample is a bi-dispersed packing with the optimum fines content. The partial void ratios can be obtained from the particle packing model (Appendix 1), and the bimodal void volumes can be obtained from Eq. (8). The permeability  $k_b$  can be determined from Eqs. (11) and (12).

The overall permeability k for the sample can be computed by  $k_a$  and  $k_b$  on a Ruess average, given by

$$\frac{h}{k} = \frac{h_a}{k_a} + \frac{h_b}{k_b} \text{ or } k = \frac{1}{\frac{1 - y_2/f_{\text{opt}}}{k_b} + \frac{y_2/f_{\text{opt}}}{k_b}}$$
(17)

Therefore, for the case of  $e_2 < 0$  representing a binary packing with a large size ratio and a low fines content, there are two ways to calculate the permeability of the sample; the percolation condition, and the non-percolation condition. Since in reality, the percolation may partially occur, thus these two conditions are the upper and lower bound of the true solution. This will be discussed later.

**Table 1** List of materials and parameters

Material type	d <sub>1</sub> (mm)	d <sub>2</sub> (mm)	$\frac{d_1}{d_2}$	$e_{1}^{0}$	$e_2^0$	η	<u>c</u> 8τ
Glass baeds [31]	3.45	0.34	3.33	0.629	0.662	1.8	0.010
	2.15	0.34	6.37	0.630	0.641	2.5	0.010
	1.13	0.34	10.22	0.646	0.667	1.8	0.010
Glass baeds [25]	0.70	0.50	1.40	0.630	0.626	1.7	0.022
	0.50	0.20	2.50	0.620	0.630	2.7	0.022
Crush sand [14]	1.09	0.15	6.75	0.890	0.820	2.7	0.008
	1.09	0.43	2.40	0.890	0.840	2.0	0.008
	1.09	0.67	1.58	0.890	0.850	2.0	0.008
Gravel sand [18]	8.00	0.40	20.00	0.488	0.751	5.0	0.020

### 3 Model evaluation

For the evaluation of the proposed model, experimental results in the literature for three types of material, glass beads, crushed sand, and gravel sand, are selected and listed in Table 1. For each type of material, several classes of binary mixtures were made of different particle size ratios. For each class of binary mixtures, several fines contents were performed for permeability tests. For all binary mixtures, the measured mono-sized void ratios for the two species are listed in Table 1. About the model prediction, the parameter  $\eta$  required for the packing density model and the coefficient  $c/(8\tau)$  required for the packing permeability model are listed for each type of binary mixtures.

### 3.1 Spherical glass beads

The model prediction is first verified with the experiments on glass beads by Mota et al. [31] and by Lee and Koo [25]. In the experiments by Mota et al. [31], glass bead mixtures were carried out with three classes of size ratios  $(d_1/d_2 = 10.22, 6.37, 3.33)$ . For each class of mixtures, the smallest particles  $(d_2 = 0.3375 \text{ mm})$  were mixing with one of the larger size particles  $(d_1 = 3.45 \text{ mm}, 2.5 \text{ mm}, \text{ and } 1.125 \text{ mm})$ . The measured and predicted void ratios of mixtures e with various fines contents are compared in Fig. 6a, c and e. The predicted variation of  $e_1$  and  $e_2$  is also plotted. The measured and predicted permeabilities with various fines content are compared in Fig. 6b, d and f.

The permeability of each specimen of the mixtures is also calculated using Kozeny-Carman equation (see Eq. (1)). For each specimen of binary mixture, d is the effective particle diameter  $d = \left(\frac{f_c}{d_2} + \frac{(1-f_c)}{d_1}\right)^{-1}$ , n is the measured porosity for the specimen, and SF is the constant



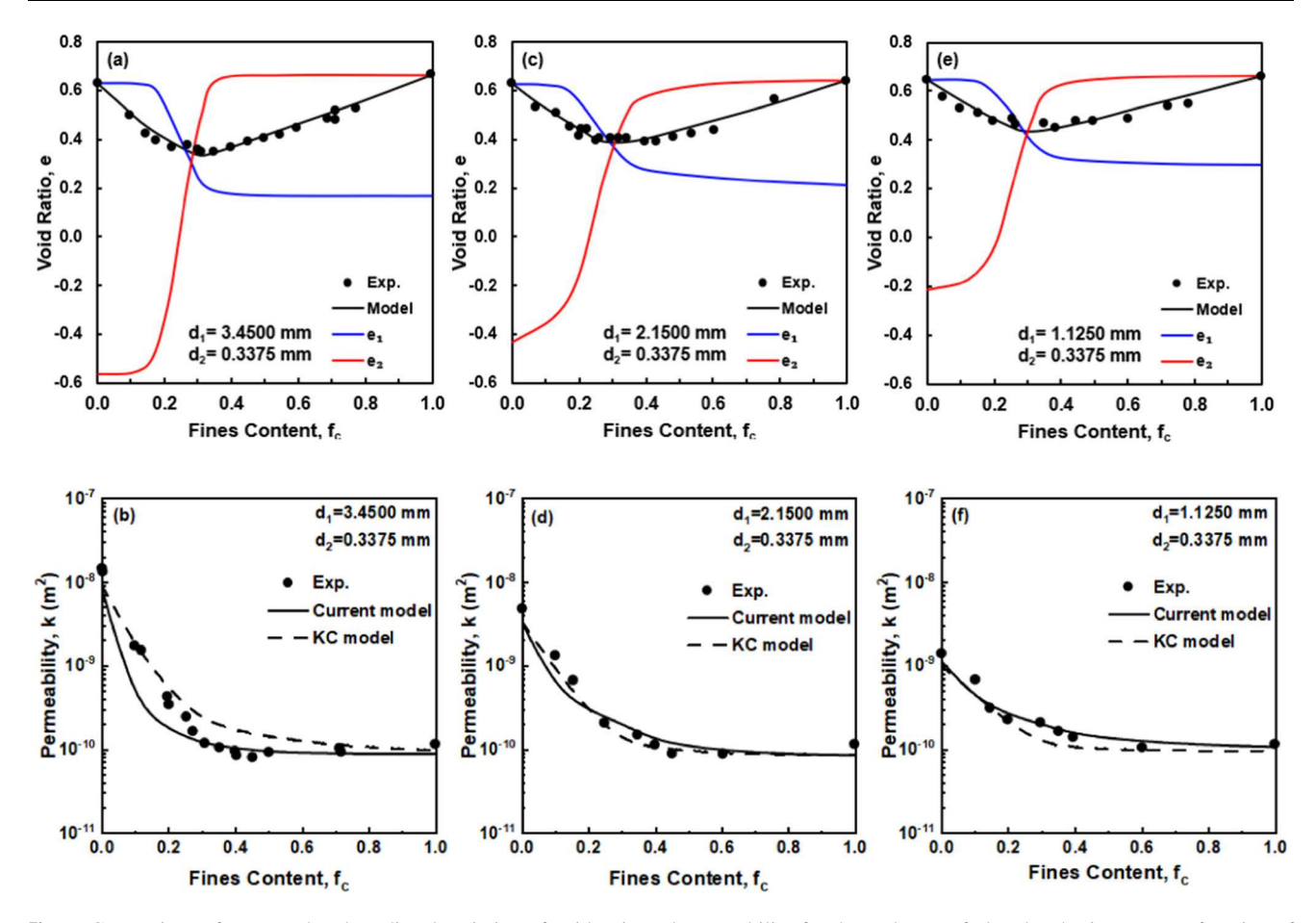


Fig. 6 Comparison of measured and predicted variation of void ratio and permeability for three classes of glass bead mixtures as a function of fines content. **a** and **b**  $d_1/d_2 = 10.22$ , **c** and **d**  $d_1/d_2 = 6.37$ , **e** and **f**  $d_1/d_2 = 3.33$  (Data from Mota et al. [31])

shape factor for all specimens of the glass bead mixtures. The value of *SF* is determined by having the calculated permeabilities of all specimens best fit to the measured data points. In Fig. 6, the value of *SF* is 6.5. The calculated permeabilities are plotted in dashed lines. Both the current model and Kozeny–Carman equation show good agreement with the measured permeabilities.

It is noted that Kozeny–Carman equation is not a predictive model because the equation demands an input parameter (porosity n), which must be physically measured for each specimen. Whereas, in the current model, the permeability is calculated from the bimodal pore sizes, which can be predicted based on the particle sizes and fines content of the specimen.

In the experiments by Lee and Koo [25], glass bead mixtures were carried out with two classes of size ratios  $(d_1/d_2 = 2.5, 1.4)$ . For each class of mixtures, particles of size 0.5 mm, mixing with particles of 0.7 mm or 0.2 mm. The measured and predicted void ratios of mixtures with various fines contents are compared in Fig. 7a and c. The predicted variation of  $e_1$  and  $e_2$  are also plotted. The

measured and predicted permeabilities with various fines contents are compared in Fig. 7b and d.

Permeabilities are also calculated using Kozeny–Carman equation (see Eq. (1)) and plotted in dashed lines. In Fig. 7, the value of *SF* is 4. Both the current model and Kozeny–Carman equation show good agreement with the measured permeabilities.

### 3.2 Crushed sands

Other than glass beads, the model prediction is verified with the experiments on crushed sand performed by Choo et al. [14], in which sands were crushed from the same parent rock and sieved into four different group of particle sizes, (1.09, 0.67, 0.43, 0.15 mm). Unlike glass beads, the particle size of the crushed sands, for each sieved group, cannot be made identical for all sand particles. Choo et al. [14] indicated that the size varies slightly with a coefficient of uniformity between 1.27 and 1.74, which is considered uniform sand. The shape also varies from particle to particle. The crushed sands are angular in shape; the roundness



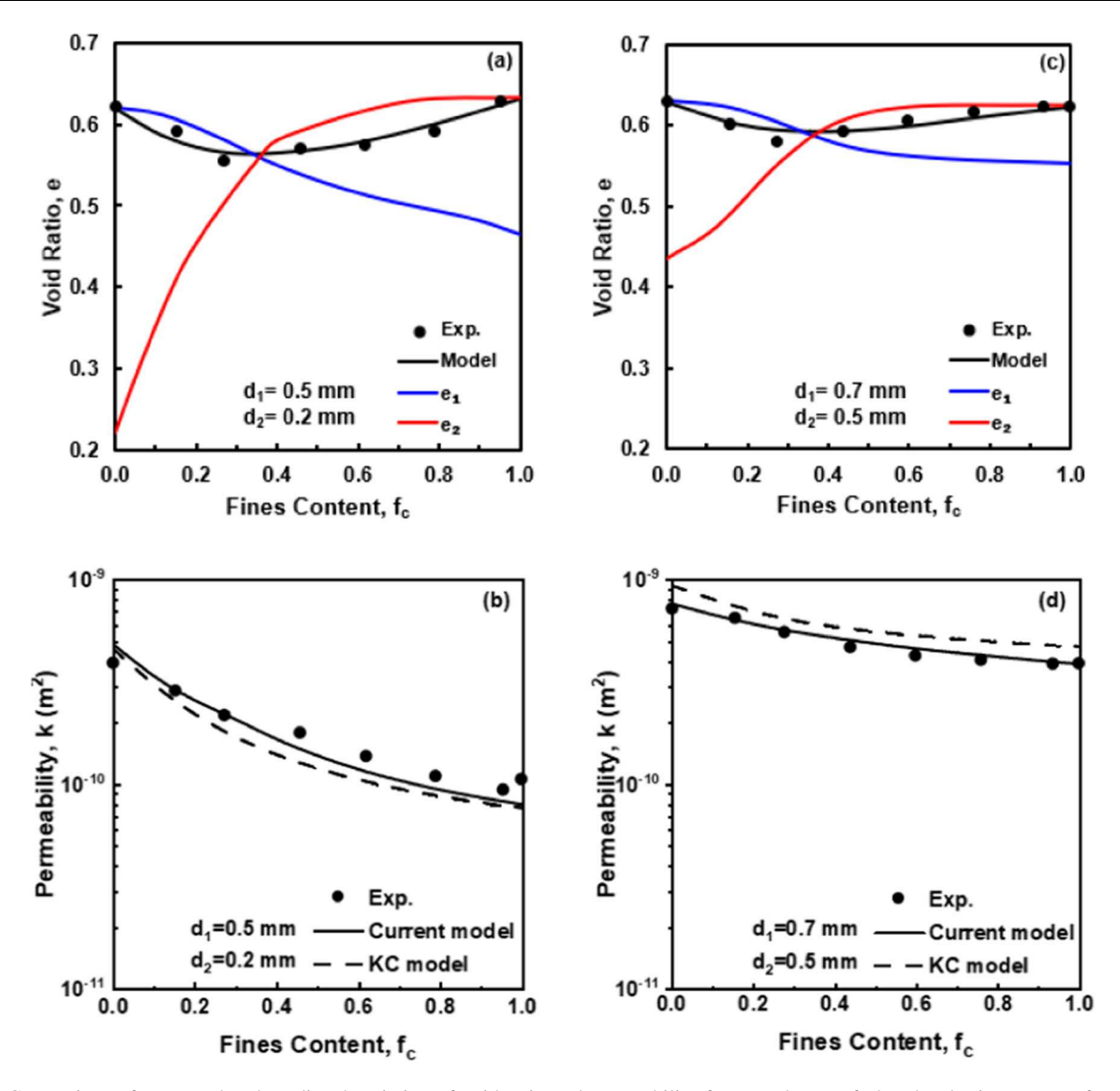


Fig. 7 Comparison of measured and predicted variation of void ratio and permeability for two classes of glass bead mixtures as a function of fines content. **a** and **b**  $d_1/d_2 = 2.5$ , **c** and **d**  $d_1/d_2 = 1.4$  (Data from Lee and Koo [25])

of tested materials range from 0.17 to 0.20 according to the method of Wadell [43].

The crushed sand mixtures were carried out with three classes of size ratio  $(d_1/d_2 = 6.75, 2.4, 1.58)$ . For each class of mixtures,  $d_1 = 1.09$  mm as the largest particles, mixing with particles of other sizes 0.67 mm, 0.43 mm, and 0.15 mm respectively. The measured and predicted void ratios of mixtures with various fines contents are compared in Fig. 8a, c and e. The variation of  $e_1$  and  $e_2$  are also plotted. The measured and predicted permeabilities with various fines contents are compared in Fig. 8b, d and f.

Permeabilities are also calculated using Kozeny-Carman equation (see Eq. (1)) and plotted in dashed lines. In Fig. 8, the value of SF is 9. Both the current model and

Kozeny–Carman equation show good agreement with the measured permeabilities.

### 3.3 Gravel sand

The model prediction is verified with the experiments by Fujikura [18] on Gravel sand. In the experiments by Fujikura [18], the size range of sand is 0.075–2 mm, and the size range of gravel is 2–26.5 mm. Each species cannot be regarded as mono-sized packing. Thus, the binary mixtures of gravel and sand with a wide range of particle sizes do not have the same meaning as bi-dispersed packing, which is supposed to be made of particles of two distinct sizes. However, Fujikura [18] considered the mean size to be 8 mm for gravel and 0.4 mm for sand. The experiments



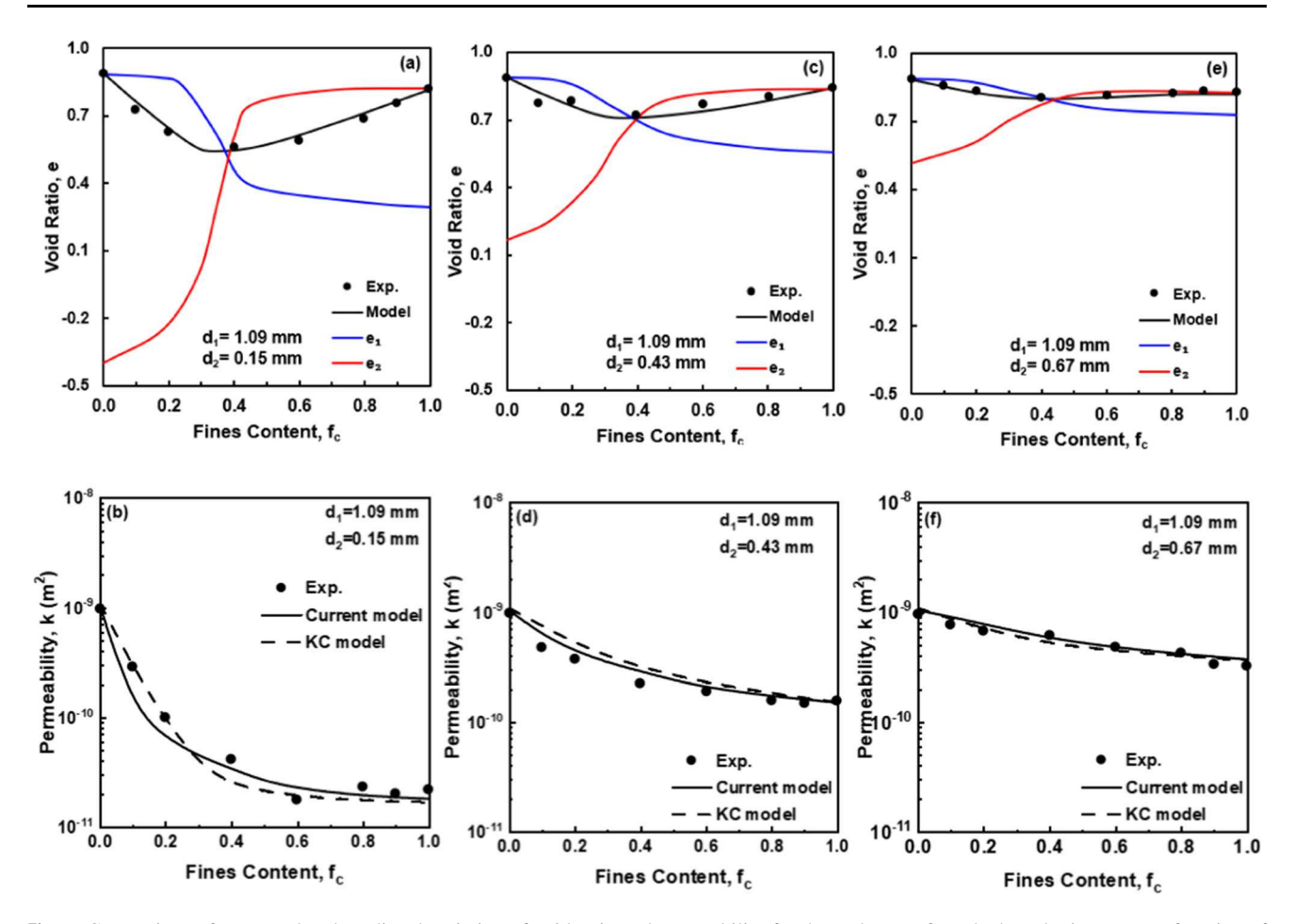


Fig. 8 Comparison of measured and predicted variation of void ratio and permeability for three classes of crushed sand mixtures as a function of fines content. a and b  $d_1/d_2 = 6.75$ , c and d  $d_1/d_2 = 2.4$ , e and f  $d_1/d_2 = 1.58$  (Data from Choo et al. [14])

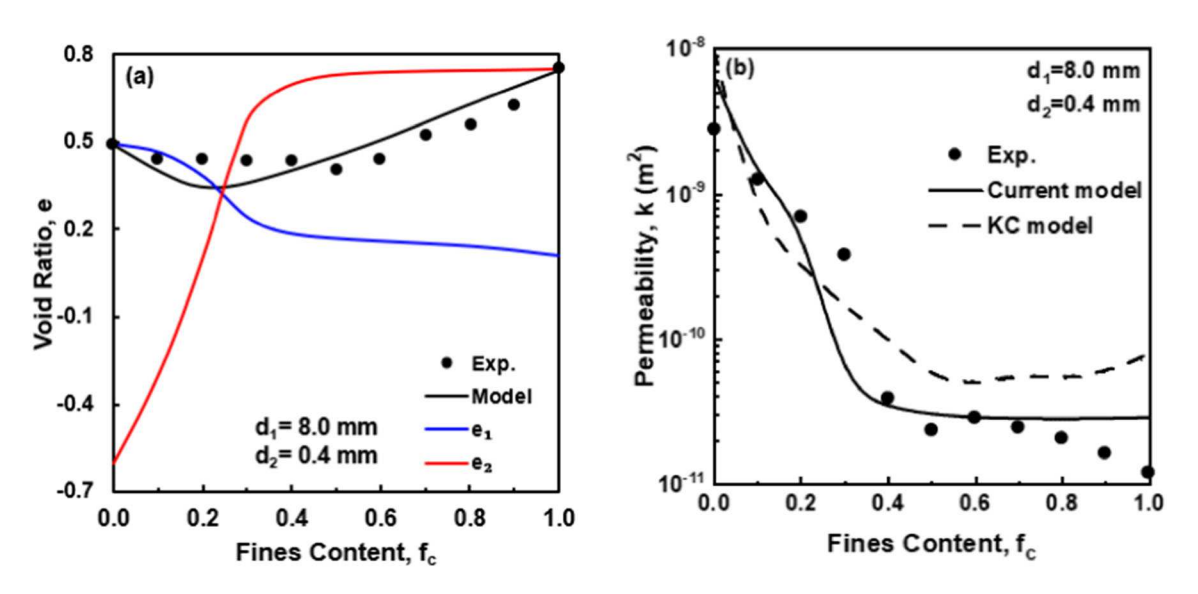
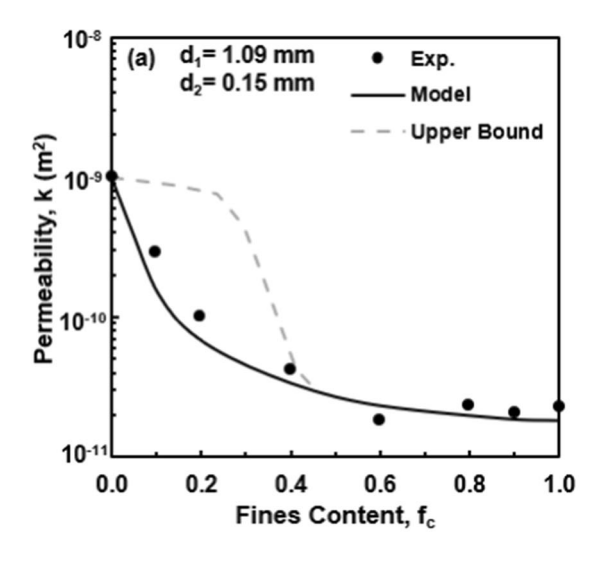


Fig. 9 Comparison of measured and predicted variation of void ratio and permeability for gravel sand mixtures as a function of fines content. (Data from Fujikura [18])





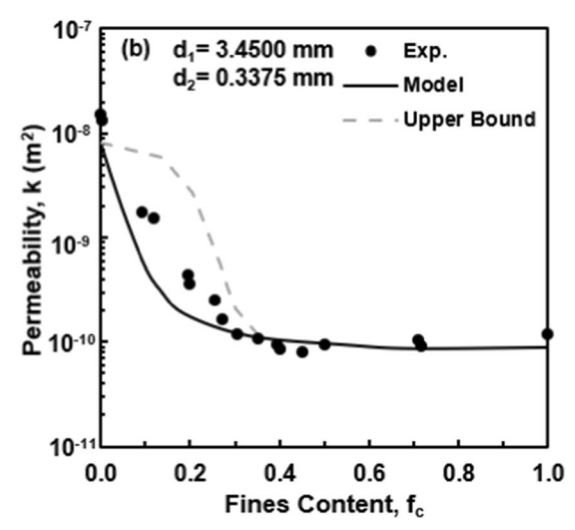


Fig. 10 The upper bound solution for the permeability of bi-dispersed packings with a large particle size ratio. a crushed sand (Choo et al. [14]) b glass beads (Mota [31])

were carried out treating the mixtures were bi-dispersed packings.

The sand and gravel are sub-round in shape. Using the mean particle sizes, the gravel sand mixtures have a size ratio  $d_1/d_2 = 20$ . The measured and predicted void ratios of mixtures with various fines contents are compared in Fig. 9a. The computed  $e_1$  and  $e_2$  is also plotted. The measured and predicted permeabilities with various fines contents are compared in Fig. 9b.

Comparing the predicted and measured results, the agreement is not as good as in the previous cases. However, the trend is well captured. The disagreement may be due to the wide particle size range for each species.

Permeabilities are also calculated using Kozeny–Carman equation (see Eq. (1)) and plotted in dashed lines. In Fig. 9, the value of *SF* is 10. Both the current model and Kozeny–Carman equation show reasonably good agreement with the measured permeabilities. It is noted that in Fig. 9a, the measured void ratio of sand is much higher than that of gravel, thus the porosity increases rapidly when the volume fraction of sand is dominant (i.e., fines content greater than 0.6). Therefore, the permeabilities calculated using Kozeny–Carman equation show an increasing trend in the range of fines content greater than 0.6, which seems to be unrealistic. On the other hand, the unrealistic trend is not shown in the current model because the current model calculated permeability based on the bimodal pore sizes, rather than the porosity, of a mixture.

### 4 Discussion

In all above predictions, the value of  $c/(8\tau)$  in Eq. (11) is assumed to be a constant for each material type. With this assumption, the predicted and measured results show very good agreement for binary mixtures with various fines contents and particle size ratios. The value of  $c/(8\tau)$  is 0.01 for the glass beads tested by Mota et.al. [31], 0.022 for the glass beads tested by Lee and Koo [25], 0.008 for crushed sand [14] and 0.002 for gravel sand [18]. The range of  $c/(8\tau)$  varies from 0.002 to 0.022, which reflects the factor of tortuosity/particle shape for different material type. However, for a given material type, the applicability of using a constant  $c/(8\tau)$  indicates that, the variation of fines content and particle size ratio has insignificant effect on the factor of tortuosity/particle shape. Thus, for a given material type, the permeability is primarily influenced by the effective void size.

For binary packings with high particle size ratios, the packing structure at low fines content would cause the partial void ratio  $e_2 < 0$ , and the packing tends to have some degree of particle percolation during the permeability tests. If the non-percolation case is assumed, the predicted permeability would be much higher than the measured results as shown by the dash lines in Fig. 10.

Thus, the upper bound is the non-percolation case. The lower bound is the complete percolation case with two distinct parts of the sample as shown in Fig. 5. It is noted that all the model predictions shown in the previous section are based on the assumption of complete percolation. Therefore, the analyses show that high degree of particle percolation has occurred on all the cases with  $e_2 < 0$ . Hence, percolation is a more realistic assumption for



predicting permeability of binary mixtures with high particle size ratios.

The developed model is capable of predicting the bimodal pore sizes of a specific assembly of granular mixture with any given fines content. The prediction is based on the void ratios  $(e_1^0 \text{ and } e_2^0)$ , which are measured, at a specified compaction level, separately for the mono-sized packings of large particles and small particles. Thus, the assembly of granular mixture must be regarded to have the same specified compaction level as the mono-sized packings, in order for the prediction of bimodal pore sizes to be valid.

Consequently, in the analysis of permeabilities using the developed model, the specimens of various fines content must be compacted at the same compaction level. In this study, the specimens of crushed sand mixture and gravel-sand mixture were compacted to the same relative densities [14, 18]. For the specimens of glass bead mixtures, relative densities were not measured, but the specimens were compacted using the same preparation procedure [25, 31].

### 5 Conclusion

There are two goals of the current study. The first goal was to develop a model for the bimodal void size distribution predicted from the particle size distribution of a binary mixture of soil. The second goal was to develop the permeability of the binary soil mixture based on the bimodal void size distribution.

The conclusion of this study is listed below:

- The applicability of the developed model is demonstrated by comparing the predicted and measured permeabilities for binary mixtures of glass beads, crushed sand, gravel sand.
- 2. This model can be used for materials made of two types of non-plastic soil particles, such as sand and gravel. The model is restricted by the following conditions: (1) the size ratio of the two types of particles should not exceed 20, and (2) all specimens must be prepared at the same compaction level.
- 3. The conventional Kozeny–Carman model is not a predictive model for binary mixtures, because the porosity of each specimen needs to be physically measured as an input parameter. Whereas, the developed model predicts permeability based on the bimodal pore sizes, which can be predicted with particle sizes and fines content. Thus, it can be used as a tool to predict permeabilities for binary mixtures.
- 4. The concept of partial void ratios [11] is useful for predicting the evolution of pore sizes with respect to the variation of fines content. The magnitudes of

calculated partial void ratios are also useful for identifying the condition of particle percolation, which allows more precise and realistic analysis.

# Appendix 1: A brief summary of a particle packing model by Chang and Deng [11]

In the model derivation for particle packing of binary mixtures, specific volume v was used. By definition, specific volume v is related to void ratio e by v = 1 + e. Thus, the equations in the derivation for the specific volume of a binary packing mixture can be replaced by the void ratio, which is a function of the solid fractions of species  $(y_1, y_2)$  and the partial void ratios, given by

$$e = e_1 y_1 + e_2 y_2 \tag{18}$$

Based on the concept of excess particle volume-potential for each species in a mixture [11], the partial void ratios of the two species in a granular mixture were postulated to be:

$$e_1 = e_1^0 - \alpha_1 (e_1^0 - 1) \tag{19}$$

$$e_2 = e_2^0 - \alpha_2 e_2^0 \tag{20}$$

where  $e_1^0$  and  $e_2^0$  are respectively the mono-sized void ratios of the two species. The values of two activity coefficients  $\alpha_1$ ,  $\alpha_2$  are between 0 and 1. With Eqs. (18), (19), and (20), the void ratio of the mixture can be expressed as:

$$e = (e_1^0 - \alpha_1(e_1^0 - 1))y_1 + (1 - \alpha_2)e_2^0y_2$$
 (21)

The activity coefficients  $\alpha_i$  is hypothesized to be a function of the two characteristic lengths in the form of power law, given by

$$\alpha_1 = \left(1 - \frac{x}{d_1}\right)^{\eta}; \alpha_2 = \left(1 - \frac{d_2}{x}\right)^{\eta}$$
 (22)

where  $d_1$  and  $d_2$  are the particle size of the two species, x is the characteristic length of the packing and  $\eta$  is a material coefficient.

Based on the thermodynamics second law, the excess volume potential must be minimized at equilibrium of the system, thus it leads to

$$\frac{\partial \alpha_1(x)}{\partial x}(e_1^0 - 1)y_1 + \frac{\partial \alpha_2(x)}{\partial x}e_2^0y_2 = 0$$
(23)

The unknown variables,  $\alpha_1$ ,  $\alpha_2$  and x can be solved by Eqs. (22) and (23). Then, the void ratio e of the binary mixture can be determined from Eq. (21). The partial void ratios can be determined from Eqs. (19) and (20).



**Acknowledgements** The first author was supported by the National Science Foundation of the United States under a research grant (CMMI-1917238). The support is gratefully acknowledged.

**Data availability** All data generated or analyzed during this study are included in this published article.

### References

- Alyamani MS, Sen Z (1993) Determination of hydraulic conductivity from complete grain-size distribution curves. Ground Water 31(4):551–555
- Arya LM, Paris JF (1981) A physico-empirical model to predict the soil moisture characteristic from particle size distribution and bulk density data. Soil Sci Soc Am J 45(6):1023–1030. https:// doi.org/10.2136/sssaj1981.03615995004500060004x
- 3. Bear J (1988) Dynamics of fluids in porous media. Dover Publications, New York
- Blunt MJ (2017) Multiphase Flow in Permeable. Media. https://doi.org/10.1017/9781316145098
- Bodman GB, Constantin GK (1965) Influence of particle size distribution in soil compaction. Hilgardia 36(15):567–591. https://doi.org/10.3733/hilg.v36n15p567
- Budhu M (2008) Soil mechanics and foundations. Wiley, New York
- Burdine NT (1953) Relative permeability calculations from pore size distribution data. J Pet Technol 5:71–78. https://doi.org/10. 2118/225-G
- Carman PC (1937) Fluid flow through granular beds. Trans Inst Chem Eng 15:150–166
- Carrier WD (2003) Goodbye, Hazen Hello, Kozeny-Carman.
   J Geotech Geoenviron Eng 129(11):1054–1056. https://doi.org/ 10.1061/(ASCE)1090-0241
- Chang CS (2022) Jamming density and volume-potential of a bidispersed granular system. Geophys Res Lett. https://doi.org/10. 1029/2022GL098678
- Chang CS, Deng Y (2022) Compaction of bi-dispersed granular packing: analogy with chemical thermodynamics. Granul Matter. https://doi.org/10.1007/s10035-022-01219-5
- Chapuis RP (2004) Predicting the saturated hydraulic conductivity of sand and gravel using effective diameter and void ratio.
   Can Geotech J 41(5):787–795. https://doi.org/10.1139/t04-022
- Chapuis RP, Aubertin M (2003) On the use of the Kozeny– Carman equation to predict the hydraulic conductivity of soils. Can Geotech J 40(3):616–628
- Choo H, Lee W, Lee C, Burns SE (2018) Estimating porosity and particle size for hydraulic conductivity of binary mixed soils containing two different-sized silica particles. J Geotech Geoenviron Eng. https://doi.org/10.1061/(ASCE)GT.1943-5606. 0001802
- Costa A (2006) Permeability-porosity relationship: a reexamination of the Kozeny–Carman equation based on a fractal porespace geometry assumption. Geophys Res Lett 33(2):L02318
- 16. Das BM (2008) Advanced soil mechanics. CRC Press, New York
- Freeze RA, Cherry JA (1979) Groundwater. Prentice Hall, Englewood Cliffs
- Fujikura Y (2019) Estimation of permeability for sand and gravel based on pore-size distribution model. J Mater Civ Eng. https:// doi.org/10.1061/(ASCE)MT.1943-5533.0002945
- Gao QF, Zhao D, Zeng L, Dong H (2019) A pore size distribution-based microscopic model for evaluating the permeability of clay. KSCE J Civ Eng 23(12):5002–5011. https://doi.org/10.1007/s12205-019-2219-z

- Hazen A (1911) Discussion of dams on sand foundations by A.
   Koenig, vol 73. Transaction ASCE, New York, pp 199–203
- Hwang S, Powers SE (2003) Lognormal distribution model for estimating soil water retention curves for sandy soils. Soil Sci 168(3):156–166
- Juang CH, Holtz RD (1986) A probabilistic permeability model and the pore size density function. Int J Numer Anal Methods Geomech 10(5):543–553
- Koohmishi M, Azarhoosh A (2021) Assessment of permeability of granular drainage layer considering particle size and air void distribution. Constr Build Mater 270:121373. https://doi.org/10. 1016/j.conbuildmat.2020.121373
- Kozeny J (1927) Über Kapillare Leitung des Wassers im Boden. Sitzungsber Akad Wiss Wien 136:271–306
- Lee H, Koo S (2014) Liquid permeability of packed bed with binary mixture of particles. J Ind Eng Chem 20:1937–1401. https://doi.org/10.1016/j.jiec.2013.07.024
- Loudon AG (1952) The computation of permeability from simple soil tests. Geotechnique 3(4):165–183. https://doi.org/10.1680/ geot.1952.3.4.165
- Mitchell JK (1976) Fundamentals of soil behaviour. John Wiley, New York
- Mitchell JK, Soga K (2005) Fundamentals of soil behavior. John Wiley and Sons, Hoboken, NJ
- Mokwa RL, Trimble NR (2008) Permeability of coarse-grain soil from void space and pore distribution. In: Proceedings of GeoCongress 2008: characterization, monitoring, and modeling of geosystems, pp 428–435. https://doi.org/10.1061/ 40972(311)54
- Mortensen N, Okkels F, Bruus H (2005) Reexamination of Hagen–Poiseuille flow: shape dependence of the hydraulic resistance in microchannels. Phys Rev E. https://doi.org/10.1103/ PhysRevE.71.057301
- Mota M, Teixeira JA, Bowen WR, Yelshin A (2001) Binary spherical particle mixed beds: Porosity and permeability relationship measurement. Trans Filtr Soc 1(4):101–106
- NAVFAC (Naval Facilities Engineering Command) (1974) Soil mechanics, foundations, and earth structures. Design Manual DM7. US Government Printing Office, Washington
- O'Sullivan C, Bluthé J, Sejpar K, Shire T, Cheung LYG (2015)
   Contact based void partitioning to assess filtration properties in DEM simulations. Comput Geotech 64:120–131. https://doi.org/ 10.1016/j.compgeo.2014.11.003
- Riva M, Sanchez-Vila X, Guadagnini A (2014) Estimation of spatial covariance of log conductivity from particle size data. Water Resour Res 50(6):5298–5308. https://doi.org/10.1002/ 2014WR015566
- Roozbahani MM, Borela R, Frost D (2017) Pore size distribution in granular material microstructure. Materials 10:1237. https://doi.org/10.3390/ma10111237
- Rosas J, Lopez O, Missimer TM, Coulibaly KM, Dehwah AHA, Sesler K, Lujan LR, Mantilla D (2014) Determination of hydraulic conductivity from grain-Size distribution for different depositional environments. Ground Water 52(3):399–413. https:// doi.org/10.1111/gwat.12078
- Sangani AS, Acrivos A (1982) Slow flow past periodic arrays of cylinders with application to heat transfer. Int J Multiph Flow 8(3):193–206
- 38. Silbey RJ, Alberty RA, Bawendi MG (2005) Physical chemistry, 4th edn. John Wiley & Sons Inc, Hoboken
- Taylor HF, O'Sullivan C, Sim WW (2015) A new method to identify void constrictions in micro-CT images of sand. Comput Geotech 69:279–290. https://doi.org/10.1016/j.compgeo.2015.05.
- Terzaghi K, Peck RB (1948) Soil mechanics in engineering practice. Wiley, New York



- Thevanayagam S (1998) Effect of fines and confining stress on undrained shear strength of silty sands. J Geotech Geoenviron Eng 124(6):479–491
- Thies-Weesie DME, Philpse AP (1994) Liquid permeation of bidisperse colloidal hard-sphere packings and the Kozeny–Carman scaling relation. J Colloid Interface Sci 162:470–480. https:// doi.org/10.1006/jcis.1994.1062
- 43. Wadell H (1935) Volume, shape, and roundness of quartz particles. J Geol 43(3):250–280
- 44. Wang J-P, François B, Lambert P (2017) Equations for hydraulic conductivity estimation from particle size distribution: a dimensional analysis. Water Resour Res 53(9):8127–8134. https://doi.org/10.1002/2017WR020888
- Yilmaz Y (2009) A study on the limit void ratio characteristics of medium to fine mixed graded sands. Eng Geol 104:290–294. https://doi.org/10.1016/j.enggeo.2008.11.009

 Zick AA, Homsy GM (1982) Stokes flow through periodic arrays of spheres. J Fluid Mech 115:13–26. https://doi.org/10.1017/ S0022112082000627

**Publisher's Note** Springer Nature remains neutral with regard to jurisdictional claims in published maps and institutional affiliations.

Springer Nature or its licensor (e.g. a society or other partner) holds exclusive rights to this article under a publishing agreement with the author(s) or other rightsholder(s); author self-archiving of the accepted manuscript version of this article is solely governed by the terms of such publishing agreement and applicable law.

